PROCEEDINGS OF SCIENCE
ONLINE ICRC 2021 THE ASTROPARTICLE PHYSICS CONFERENCE Berlin | Germany
37th International Cosmic Ray Conference 12–23 July 2021

Supernova remnants of a 60 $M_\odot$ massive star

D. M.-A. Meyer,[a,*] M. Petrov[b] and M. Pohl[a,c]

[a] *Institut für Physik und Astronomie, Universität Potsdam, Karl-Liebknecht-Strasse 24/25, 14476 Potsdam, Germany*
[b] *Max Planck Computing and Data Facility (MPCDF), Gießenbachstrasse 2, D-85748 Garching, Germany*
[c] *DESY Platanenallee 6, D-15738 Zeuthen, Germany*
E-mail: dmameyer.astro@gmail.com

The initial mass function predicts that very few massive stars can have a zero-age-main-sequence mass exceeding 60 $M_\odot$. These rare objects can evolve to exotic phases of stellar evolution, such as the Luminous-Blue-Variable and Wolf-Rayet phases, and might finish their lives via a core-collapse supernova explosion. We present 2D axisymmetric hydrodynamical simulations of the surroundings of such very massive stars, characterised by both a high mass-loss rate and by strong wind velocities. We found that it is shaped as a 100 pc large stellar wind bubble. In the context of a fast-moving stellar motion of the order of $\sim$ 20-40 $\mathrm{km\,s^{-1}}$, into the warm phase of the interstellar medium (ISM), these stars can escape their own circumstellar bubble. The location of the supernova explosion, where the star dies, is therefore off-set to the geometrical center of its pre-supernova circumstellar nebula, and, as a consequence, the subsequent supernova remnant reflects the asymmetries of the shaped medium. We find that the formed, distorted, cavity of stellar wind in which the enriched supernova ejecta expand hosts an efficient mixing of stellar wind and ISM materials. We propose that peculiar enrichment of the ISM can be used as a tracer of the runaway nature of the high-mass stellar progenitors of these supernova remnants.

37th International Cosmic Ray Conference (ICRC 2021)
July 12th – 23rd, 2021
Online – Berlin, Germany

*Presenter

PoS(ICRC2021)983

1. Introduction

High-mass stars ($M_{\star} \geq 8\,\mathrm{M}_{\odot}$) are rare stellar objects of huge importance in the cycle of matter of our Galaxy. The fast, dense and enriched stellar winds expelled from their surface replenish the interstellar medium (ISM) with momentum, energy and heavy chemical elements. The wind-ISM interaction of these main-sequence massive stars form huge parsec-scale large circumstellar wind bubbles, which classical description can be found in [1]. These nebula are composed of an inner termination shock and an outer forward shock, respectively, which encompass a contact discontinuity where the hot, diluted shocked stellar wind and the cold, dense shocked ISM materials meet. Without any strong perturbation of their ambient medium, and considering a static massive star, the wind-blown bubbles grow spherically and conserve this symmetry throughout the several evolutionary phases of the massive star [2].

In the context of runaway massive stars moving supersonically through their local ISM, the symmetry of their circumstellar wind bubble is broken and it is distorted as an arc-like shape called a stellar-wind bow shock. It is constituted of layers, discontinuities and shocks similar to those in the wind bubbles forming around a static star. Such bow shocks form around about 10% of all OB-typed stars [3]. When bow-shock-carrying massive stars reach the end of their evolution and die [4, 5], their surroundings are the pre-supernova circumstellar medium in which the supernova explosion happens [6]. The interaction between the expanding supernova shock wave and the circumstellar medium of the defunct star induces deviations from sphericity to the growing supernova remnant. Famous examples are the Cygnus Loop nebula [7], Tycho's [8] and Kepler's supernova remnant [9, 10], albeit some of them involve lower-mass binary companions to the supernova progenitor. Asymmetries can also directly form during the explosion itself [11]. The main question is therefore, which high-mass stars can generate, throughout their lives, a circumstellar medium sufficiently asymmetric to generate the most aspherical remnants?

Good candidates are the very high-mass stars evolving through eruptive stellar evolutionary phases like the Luminous Blue Variable and/or Wolf-Rayet phases, both being characterised by a strong increase of the mass-loss rate and brutal changes in their wind properties. These shells and eruptive accumulation over the different post-main-sequence phases generate a complex circumstellar medium, and, as an additional effect, the bulk motion of the progenitor engenders the asymmetries and inhomogeneous cavities in which the supernova remnants of those stars develop asymmetric shapes. So-evolving massive stars nevertheless exist and have been observed in both our Galaxy and the Large Magellanic Cloud. They are believed, from the theoretical point of view, to generate distorted circumstellar nebulae and hence to produce asymmetric core-collapse supernova remnants. We investigate the effects of these consecutive post-main-sequence evolutionary phases onto the shaping of wind-blown nebulae, see also [12], and, we pay attention of the effects of the stellar motion to the remnant's morphology.

Our methods in presented in Section 2 and show our results in Section 3. We conclude in Section 4.

2. Methods

Numerical simulations are performed with the PLUTO code [13–15] in a 2D axisymmetric fashion. We use a cylindrical coordinate system, as utilised in previous studies devoted to wind-ISM calculations [12, 17], and the stellar wind is injected within the origin of the computational domain, by interpolating tabulated an evolution model of a $60\,\mathrm{M}_{\odot}$ zero-age main-sequence star [16]. Our stellar wind bubbles, generated by wind-ISM interaction, are therefore modelled using the formalism developed in the context of the circumstellar medium of massive stars, see e.g. [18]. Throughout the simulations, we solve the equations of hydrodynamics, with an additional energy loss term accounting for optically-thin radiative heating and cooling, used within a second order finite-volume scheme making use of the Harten-Lax-van Leer approximate Riemann solver. Our calculations are both performed at the Max Planck Computing and Data Facility in Garching and at the North-German Supercomputing Alliance.

We first simulate the wind-ISM interaction. The corresponding wind-blown bubble is calculated in the frame of the runaway star, moving with velocity $v_{\star}$. The ISM properties are those of the warm phase of the Galactic plane, which we initially set to a temperature of $8000\,\mathrm{K}$ for a gas number density of $0.79\,\mathrm{cm}^{-3}$, respectively. Importantly, the advection of the stellar wind gas into the ISM can be tracked and separated from the other species of that problem (ambient medium, supernova ejecta) making use of a passive scalar tracers [13, 14]. Then, we a release a core-collapse supernova blastwave in our pre-shaped medium. The early interaction of the supernova ejecta blastwave with the stellar wind is calculated with an extra one-dimensional, high-resolution simulation which we map into the 2D pre-supernova circumstellar medium [19, 20]. Our series of 3 models differ by the star's bulk motion, taken to $v_{\star} = 0\,\mathrm{km\,s}^{-1}$ (static star) to $v_{\star} = 20\,\mathrm{km\,s}^{-1}$ (runaway case), respectively.

3. Results

Fig. 1 shows the density field (in cm^{-3}) in three simulations of supernova remnants generated by a supernova explosion expanding into the pre-shaped circumstellar medium of its $60\,\mathrm{M}_{\odot}$ massive progenitor. The figures differ by the space velocity of the progenitor star, which spans from $v_{\star} = 0\,\mathrm{km\,s}^{-1}$ (panel a) to $v_{\star} = 20\,\mathrm{km\,s}^{-1}$ (panel c).

In Fig. 1a we plot the pre-supernova wind bubble of the static $60\,\mathrm{M}_{\odot}$ star in which the supernova shock wave has already started expanding. The modelled situation is the 2D equivalent of the classical picture for stellar wind bubbles [1]. The overall circumstellar structure is composed of an inner termination shock and of an outer forward shock (at radius $\sim 80\,\mathrm{pc}$), generated during the main-sequence phase of the star. The unstable contact discontinuity separates the shocked, diluted, evolved stellar wind and the shocked ISM gas swept-up during the evolution of the massive star. The expanding supernova shock wave is clearly visible in the center of at the nebula (at radius $\sim 40\,\mathrm{pc}$). The evolution of the shock wave is still spherical as it has not interacted with any dense structure, which remains far from the ejecta.

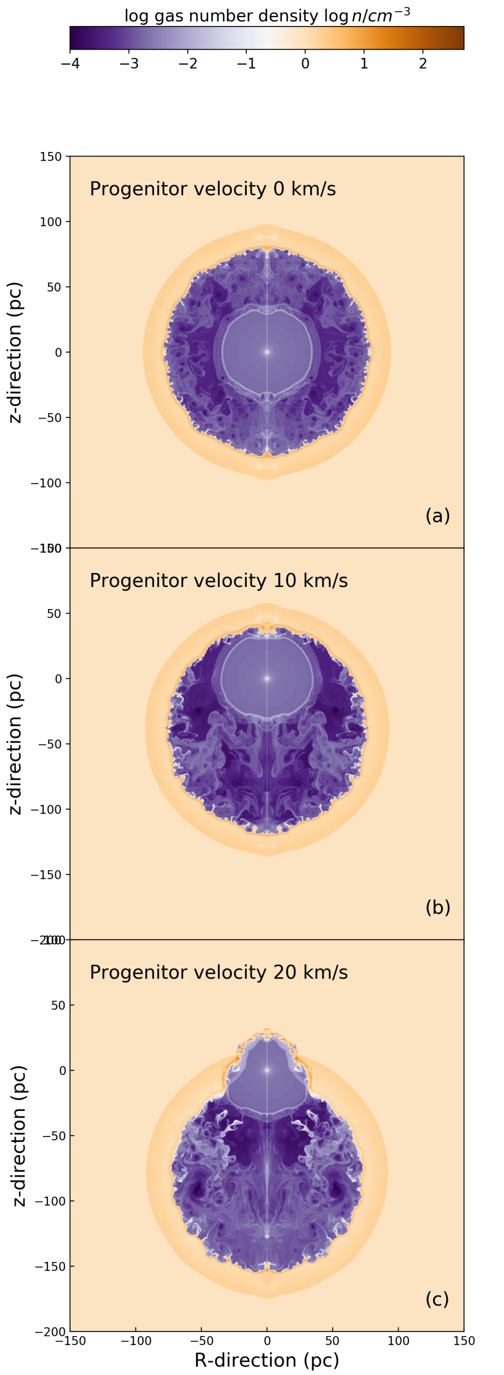

Figure 1: Density field (plotted in cm^{-3}) of the supernova remnants of a $60\,\mathrm{M}_{\odot}$ massive progenitor star, moving with velocity 0 (a), 10 (b), and $20\,\mathrm{km\,s^{-1}}$ (c).

Fig. 1b shows the density field in the supernova remnant simulation generated by a slowly-moving progenitor. The center of the explosion is shifted from the geometrical center of the wind bubble. While the remnant is as old as that of Fig. 1a, the northern part of the expanding shock wave is nearly interacting with the contact discontinuity of the stellar wind bubble, which results in mild changes in the forward shock of the blastwave. The reflection of the last Wolf-Rayet stellar wind against the wind-ISM interface is different from that in the static case, as testifies the instabilities in the turbulent material located between the blastwave and the wind-ISM interface, as well as the instabilities affecting that same interface, more pronounced in the southern part of the wind bubble. In Fig. 1c we plot the supernova remnant of a runaway progenitor moving with $20\,\mathrm{km\,s^{-1}}$, i.e. the stellar motion is supersonic with respect to the sound speed in the ISM. In this simulation, the center of the explosion is directly located in the shell of shocked ISM and main-sequence stellar wind materials, as a result of the faster space velocity of the star compare to that in models Fig. 1a,b. Hence, the expanding blastwave has already been constrained and shaped by pre-supernova gas distribution: it expands faster in the direction opposite of that of the progenitor's motion, whereas it interacts strongly with the dense bubble in the direction of stellar motion while beginning to further penetrate into the unperturbed ISM.

In Fig. 2 we show the time evolution of the mixing between stellar wind, supernova ejecta and ISM materials moving with velocity $v_{\star} = 20\,\mathrm{km\,s^{-1}}$, shown at times 10 (a), 20 (b) 40 (c) and 200 kyr (d) after the explosion, respectively. Left-hand part of each panel is the ratio of ISM gas in the each grid cell, right-hand part is that of the stellar wind material, respectively (0 means absence of a given specie, 1 indicates that the zone is exclusively made of a particular specie).

Several black (left) and white (right) contours highlight the regions in the remnant where the temperature is $T = 10^5$, 10^6, and $10^7\,\mathrm{K}$ (left), and where the gas number density with is $n = 1.0$, 10^1, 10^2, and $10^3\,\mathrm{cm}^{-3}$ (right). Moreover, the blue contours mark the regions in the remnant where the ejecta contributes 10% of the gas in number density.

Fig. 2a shows the remnant 10 kyr after the explosion, which corresponds to the number density field in Fig. 1c. The mixing of main-sequence and evolved stellar winds, together with the shocked ISM gas, affects the entire interior of the pre-supernova wind bubble (see colored particle tracer fields). Note that the central region of the wind bubble is slightly less affected by this mixing of gases, which might rely on the 2D nature of the simulations. The blue contours highlight the young region made of supernova ejecta such as the metals synthetised in the core of the stellar progenitor prior to the supernova explosion.

In Fig. 2b the shock wave has expanded in the low-density cavity of stellar wind, while it has much less progressed in the direction of stellar motion because of its ongoing interaction with the regions of shocked ISM gas. Notably, both fronts see the development of Rayleight-Taylor instabilities at the ejecta-wind and ejecta-ISM interfaces. At later times, in Fig. 2c, the progression mechanism of the supernova blastwave keeps going, as well as the mixing of stellar wind and shocked ISM materials taking place in the surrounding environment. Similarly, the generation of instabitilies at the forward shock of of the shock wave is even more pronounced, and, a small region of hot mixted ISM, stellar wind and ISM gas forms at the apex of the still runaway supernova remnant.

The last panel of the figure (Fig. 2d) highlights the supernova remnant at even much later times, 200 kyr after the supernova explosion. The supernova shock wave has largely expanded and its forward shock has reached the bottom of the cavity of stellar wind. The while structure is therefore filled with a mixture of supernova ejecta, shocked stellar wind and shocked ISM material. The efficient deceleration of the forward shock of the supernova shock wave along the direction of stellar motion makes the part of it which directly interacts with the unperturbed ambient medium almost static and the remnant does not grow much in size. Only a thin, elongated region of the interior of the supernova remnant escape from the mixing processes, and remain made of supernova ejecta exclusively. This may rely of the geometry of the calculations, and further 3D MHD models are necessary to address these question.

4. Conclusion

Our simulations demonstrate that a very massive star of initial mass $\sim 60\,\mathrm{M}_{\odot}$ can enormously impact its surroundings, with or without being animated by a stellar bulk motion regarding to its local ambient medium. The peculiar evolution of our considered massive star, undergoing both several Luminous-Blue-Variable and Wolf-Rayet episodes [16], eject circumstellar shells resulting in prokoving and/or emphasizing the asymmetric character of their circumstellar medium at the pre-supernova time. The outflows they produce might, if the star is sufficiently close to the shell of their wind bubble, pierce it and thus open a path for the subsequent shock wave of the defunct progenitor star. Inversely, static or slowly-moving stars ($\sim 10\,\mathrm{km\,s^{-1}}$) can not break the sphericity of the supernova remnant.

PoS(ICRC2021)983

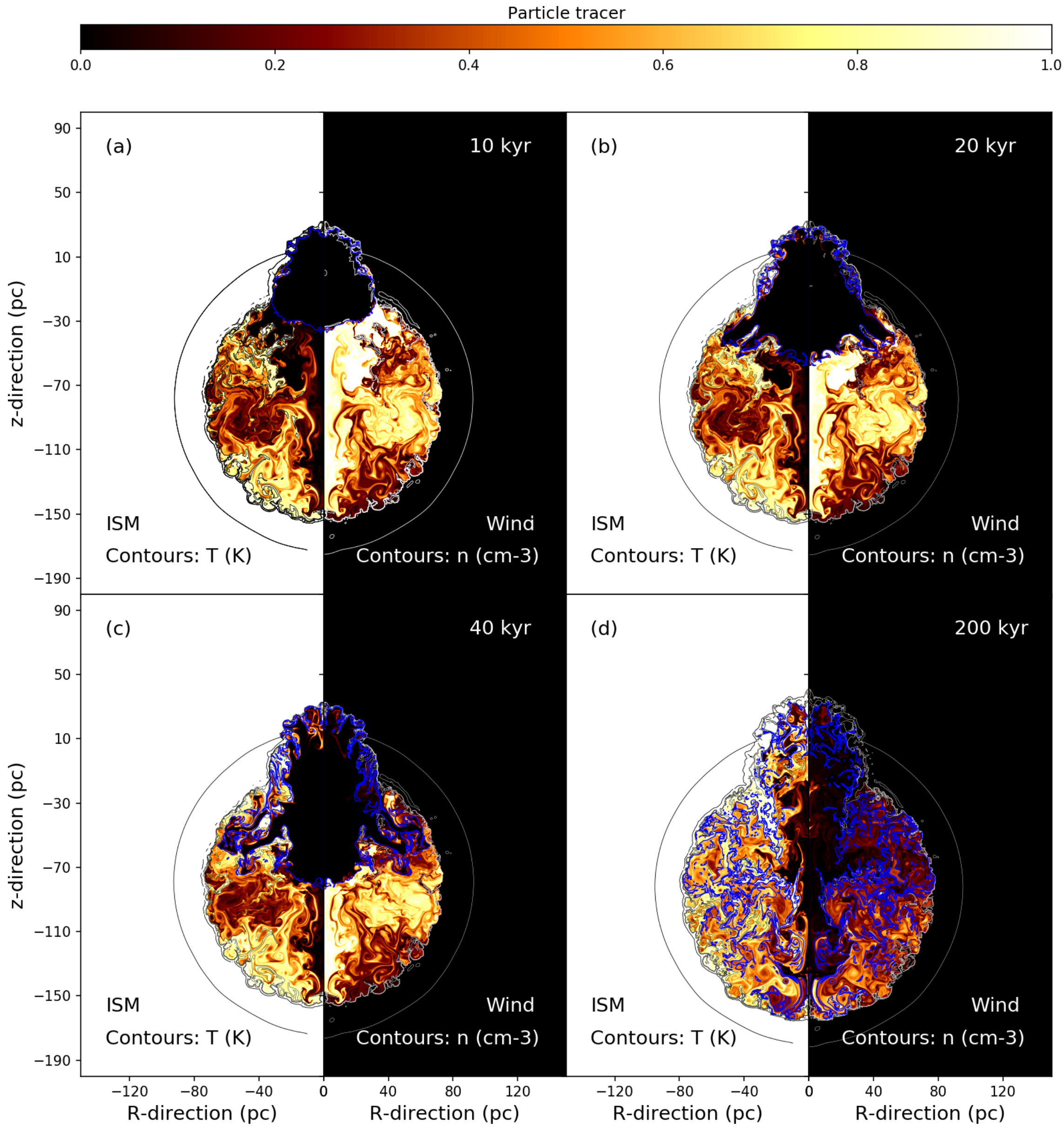

Figure 2: Supernova remnant of a $60\,\mathrm{M}_{\odot}$ star moving with velocity $20\,\mathrm{km\,s}^{-1}$ and displayed at several characteristic times of its evolution. Left-hand part of each figure is the proportion of ISM material, right-hand part is the proportion of stellar wind gas in the computational domain. Black contours are the temperature field and white contours are number density. Blue contours highlight a 10% contribution of ejecta material in number density.

The expanding supernova blastwave remains trapped and experiences several reflections inside of the layer of shocked stellar wind. Our simulations demonstrate that a unique very massive moving star is able to modify the entire gas dynamical and chemical properties of a region of the ISM. These results stress the need for investigating the chemical evolution of the surroundings of middle-age to old supernova remnants (up to 0.1 Myr), since they still bear the trace of the potential runaway nature of the dead progenitors. This problem should be further explored over a wider parameter space, for example by means of global, 3D magneto-hydrodynamical simulations.

Acknowledgement

The authors acknowledge the North-German Supercomputing Alliance (HLRN) for providing HPC resources that have contributed to the research results reported in this paper. MP acknowledges the Max Planck Computing and Data Facility (MPCDF) for providing data storage resources and HPC resources which contributed to test and optimize the PLUTO code. This research made use of the PLUTO code developed at the University of Torino by A. Mignone and collaborators, the MATPLOTLIB plotting library for the PYTHON programming language

References

[1] Weaver R., McCray R., Castor J., Shapiro P., Moore R., 1977, ApJ, 218

[2] Freyer, Tim and Hensler, Gerhard and Yorke, Harold W., 2003, ApJ, 594

[3] Gies, D. R., 1987, ApJs, 64, 545-563

[4] Gvaramadze, V. V., Menten K. M., Kniazev A. Y., Langer N., Mackey J., Kraus A., Meyer D. M.-A., Kamiński, T., 2014, Mnras, 437, 843-856

[5] Mackey J., Mohamed S., Neilson H. R., Langer N., Meyer D. M.-A., 2012, ApjL, 751, L10

[6] Franco J., Tenorio-Tagle G., Bodenheimer P., Rozyczka M., 1991, PASP, 103, 803-810

[7] Fang Jun, Yu Huan, Zhang Li, 2017, MNRAS, 464, 940-945

[8] Vigh C. D., Velázquez P. F., Gómez D. O., Reynoso E. M., Esquivel A., Matias Schneiter E., 2011, ApJ, 727, 32

[9] Chiotellis A., Schure K. M., Vink J., 2012, A&A, 537, A139

[10] Velázquez P. F., Vigh C. D., Reynoso E. M., Gómez D. O., Schneiter E. M., 2006, ApJ, 649, 779-787

[11] Toledo-Roy J. C., Esquivel A., Velázquez P. F., Reynoso E. M., 2014, MNRAS, 442, 229-238

[12] van Marle A. J., Meliani Z., Keppens R., Decin L., 2011, ApJ Letters, L26

[13] Mignone A., Bodo G., Massaglia S., Matsakos T., Tesileanu O., Zanni, C. and Ferrari, A., 2007, ApJ, 170

[14] Mignone A., Zanni C., Tzeferacos P., van Straalen B., Colella P., Bodo G., 2012, ApJs&A, 198

[15] Vaidya B., Mignone A., Bodo G., Rossi P., Massaglia S., 2018, ApJ, 865, 144

[16] Groh J. H., Meynet G., Ekström S., Georgy C., 2014, A&A, 564, A30

[17] Comerón F., Kaper L., 1998, A&A, 338

[18] Meyer D. M.-A., van Marle A.-J., Kuiper R., Kley W., 2016, MNRAS, 459

[19] Meyer D. M.-A., Langer N., Mackey J., Velázquez P. F., Gusdorf A., 2015, MNRAS, 450

[20] Meyer D. M. -A., Pohl M., Petrov M., Oskinova L. M., 2021, MNRAS 502, 4